DOI: 10.1002/ejic.200601017

Keggin POMs Modified by Bonding to Multitrack Cu(bipy) Chains through Linearly Arrayed Terminal and Bridging Oxygen Atoms of the M_3O_{13} Triad

Jingquan Sha,[a,b] Jun Peng,*[a] Hongsheng Liu,[a] Jing Chen,[a] Baoxia Dong,[a] Aixiang Tian,[a] and Zhongmin Su[a]

Keywords: Polyoxometalates / N ligands / Copper / Organic–inorganic hybrids

Two novel complexes based on the Keggin POMs modified by the Cu(4,4′-bipy) moiety, $\{[Cu(4,4'\text{-bipy})]_3[HSiMo_{12}O_{40}]\}\cdot 1.5H_2O$ (**1**) and $\{[Cu(4,4'\text{-bipy})]_4[SiW_{12}O_{40}]\}\cdot 3H_2O$ (**2**) (bipy = bipyridine), have been hydrothermally synthesized and characterized by routine physical methods and single-crystal X-ray diffraction. Complexes **1** and **2** represent the first examples of fully oxidized Keggin POM anions as pendant polydentate ligands covalently bonded to a multitrack Cu(bipy) polymer chain(s) through linearly arrayed $O_d\cdots O_c\cdots O_d$ (O_d, terminal oxygen; O_c, bridging oxygen) atoms of single M_3O_{13} triad(s). In the crystalline lattice of **1**, the 1D chain is constructed from a α-$[SiMo_{12}O_{40}]^{4-}$ ($SiMo_{12}$) cluster as a pendant tridentate ligand covalently bonded to three Cu^I(4,4′-bipy) subunits, and the neighbouring polymer strands interconnect with the Keggin fragments geared like the teeth of a zipper. In compound **2**, the 2D extended layer structure is composed of a α-$[SiW_{12}O_{40}]^{4-}$ (SiW_{12}) cluster as a pendant hexadentate ligand covalently bonded to four Cu^I(4,4′-bipy) subunits and forms a 2D net-texture structure with a large vacancy (30.9×10.6 Å), and the 2D layers are arranged in a parallel staggering fashion to form a 3D framework.

Introduction

Polyoxometalates (POMs) composed of early transition metals (V, Nb, Ta, Mo, W) have been investigated for over a century because of their intriguing structural chemistry, unexpected reactivities, and potential applications.[1] Among a wide variety of POMs, the Keggin species $[XM_{12}O_{40}]^{n-}$ (X = B, P, Si, etc.; M = Mo and W) are one of the most important research topics, especially the modified Keggin derivatives. This reflects a current interest for the following reasons: the Keggin species are viewed as soluble metal oxide analogues and can therefore be used for the modeling of catalytic reactions taking place at metal oxide surfaces; they are valuable building blocks for tailor-made inorganic and organic or metal–organic hybrid materials with attractive structures and properties.[2] The increasing attention is currently devoted to their organometallic derivatives, and their multigraft modification could prove interesting in the context of the development of multidimensional framework structures.[3] Recently, a number of Keggin POMs covalently modified by transition-metal complexes have been reported, such as the mixed-valent compounds $[\{Cu_4(terpy)_4(PO_4)(H_2O)_2\}\{W^{VI}_{10}W^{V}_{2}O_{36}(PO_4)\}]\cdot 5H_2O$ described by Zubieta et al.,[4] $[PW_{12}O_{40}\cdot Ni(2,2\text{-bipy})_2(H_2O)]^{3-}$ by Xu et al.,[5] and $(NH_4)[Cu_{24}I_{10}L_{12}][PMo^{V}_{2}Mo^{VI}_{10}O_{40}]_3$ by Wang et al.;[6] the controlled assembly from lacunary Keggin POMs has also been reported by Pope et al.[7] and Gutiérrez-Zorrilla et al.[8] All these compounds featured sufficient charge density on the Keggin anion surface atoms to coordinate the transition-metal complexes. It is believed that surface activation is achieved by reducing the metal centres or by replacing metal centre(s) with a high oxidation state by other lower-valence metal(s). However, there are only a few examples of fully oxidized Keggin POMs modified by transition-metal complexes. These examples include the unsymmetrical discrete complex $[\{Cu_2(O_2CMe)_2(5,5\text{-dimethyl-2,2-bipy})_2\}\{Cu(5,5'\text{-dimethyl-2,2'-bipy})_2\}SiW_{12}O_{40}]$,[9] the 1D framework $[Ag_3(2,4'\text{-bipy})_3PMo_{12}O_{40}]$,[10] the 3D framework complexes $[Cu_3(pz)_3(PW_{12}O_{40})]$,[11] $[Ag_3(pz)_3(PW_{12}O_{40})]$,[11] $[Ag(4,4\text{-bipy})](OH)[\{Ag(4,4\text{-bipy})\}_2\{PAgW_{12}O_{40}\}]$,[12] and $KH_2[(D\text{-}C_5H_8NO_2)_4(H_2O)Cu_3][BW_{12}O_{40}]$.[13] In the last framework, chirality was designed into the helical motif. The coordination fashions of the Keggin POMs as polydentate ligands in these complexes are graphically summarized in Scheme 1: Keggin POMs provide only a terminal oxygen atom (see Scheme 1a, e and f) or both terminal and bridging oxygen atoms (see Scheme 1b–d).

[a] Key Laboratory of Polyoxometalate Science of Ministry of Education, Faculty of Chemistry, Northeast Normal University,
Changchun, Jilin 130024, P. R. China
E-mail: jpeng@nenu.edu.cn
pjun56@yahoo.com
[b] Faculty of Chemistry and Pharmacy, Jiamusi University, Jiamusi, HeilongJiang 154007, P.R. China

Supporting information for this article is available on the WWW under http://www.eurjic.org or from the author.

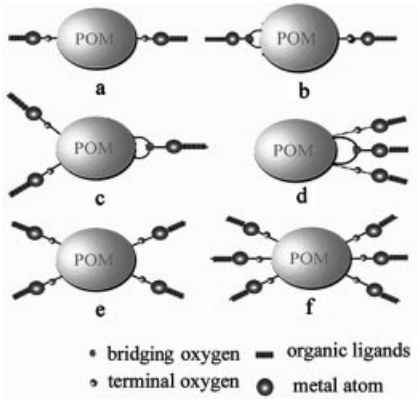

Scheme 1. Schematic representation of the coordination fashions of Keggin POMs as polydentate ligands.

It is noteworthy that most of these coordination fashions are prone to barycentre distribution of their oxo ligands, presumably because of steric crowding, with the exception of that shown in Scheme 1d, in which all the oxo ligands belong to a single M_3O_{13} triad. To the best of our knowledge, the title compounds are unique examples with the coordination fashion represented in Scheme 1d. The ligand 4,4′-bipy is a rod-like molecule and is commonly used as a rigid ligand. The d^{10} ions, the soft Lewis acid metal ions, generally show variable coordination numbers and tunable coordination spheres. Especially, Cu–bipy complex units have been widely used in magnetic and catalytic materials,[14] and some POM-based Cu–bipy polymers with interesting structures have been reported quite recently.[15] Hydrothermal synthesis represents a fast and excellent method to afford new POM structures. Although the hydrothermal synthesis employing the usual mixture of polyoxometalate, transition-metal salt, and nitrogen-containing ligand has been intensively extended, there is still abundant scope for the construction of intricate structures for new materials. The challenge is really to demonstrate control and expendability, to optimise the physical properties, etc. In this paper, we select the ligand 4,4′-bipy and the Cu ion to build metal–organic complex subunits in the hope of forming an extended structure of Keggin POMs modified by transition-metal complex moieties with little steric crowding, and we report the hydrothermal syntheses and crystal structures of two novel Cu(4,4′-bipy) modified Keggin derivatives, $[\{Cu(4,4'\text{-bipy})\}_3\{\alpha\text{-}HSiMo_{12}O_{40}\}]\cdot 1.5H_2O$ (**1**) and $[\{Cu(4,4'\text{-bipy})\}_4\{\alpha\text{-}SiW_{12}O_{40}\}]\cdot 3H_2O$ (**2**). They are the first examples of fully oxidized Keggin POM anions as pendant polydentate ligands covalently bonded to colinear multitrack Cu(bipy) chain(s) through $O_d\cdots O_c\cdots O_d$ atoms of M_3O_{13} triad(s).

Results and Discussion

The isolation of compounds **1** and **2** depends on the use of hydrothermal techniques. Hydrothermal reactions in the presence of organic ligand molecules have been established as a versatile method for the isolation of new materials with diverse structural architectures. Therefore, the introduction of hydrothermal techniques and the direct use of saturated Keggin POM as building blocks may produce a large number of novel organic–inorganic hybrid materials. By many parallel experiments, we found that the choice of starting materials is vital for the success of these reactions among other factors such as stoichiometry, temperature, pH and fill volume.[10,11] Transition-metal ions can greatly influence the structural formation of materials. We found that when $Cu(NO_3)_2\cdot 3H_2O$ was replaced by $Zn(NO_3)_2\cdot 6H_2O$, $NiCl_2\cdot 6H_2O$ or $MnCl_2\cdot 4H_2O$ in parallel experiments, we could not obtain the expected homologies but rather POM–4,4′-bipy supramolecular compounds. The oxidation states of the copper atoms in **1** and **2** are assigned as +1 on the basis of charge neutrality, coordination environments, valence sum calculations and XPS. A similar case of $Cu^{II}\rightarrow Cu^{I}$ was also observed in other polyoxometalates bridged by organonitrogen ligands coordinated to copper ions.[16] Additionally, the organic reductant species was also crucial for maintaining the intact skeleton of presynthesized saturated Keggin POMs. If the reducibility of the organic reductant were high, the skeleton of the saturated Keggin cluster may be inclined to decompose and reassemble into a new cluster.[17] We found that triethylamine was a good candidate.

Structural Description of 1

Single-crystal X-ray diffraction analysis reveals that **1** consists of one $[SiMo_{12}O_{40}]^{4-}$ anion, three $[Cu(4,4'\text{-bipy})]^{+}$ moieties and one and a half water molecules (Figure 1). The heteropolyanion $[SiMo_{12}O_{40}]^{4-}$ possesses the classical α-Keggin-type structure without disorder.[18] The tetrahedrally coordinated Si is surrounded by four oxygen atoms with Si–O bonds ranging from 1.624(7) to 1.631(8) Å (mean 1.627 Å). All Mo atoms have $\{MoO_6\}$ octahedral environments. The distances of Mo–O bonds are divided into three groups: Mo–O_a (centre oxygen atom), 2.316(7)–2.386(8) Å; Mo–$O_{b/c}$ (bridging oxygen atom), 1.821(8)–2.015(8) Å; Mo–O_d (terminal oxygen atom), 1.660(9)–1.714(8) Å.

Each $\alpha\text{-}SiMo_{12}O_{40}$ cluster as a tridentate pendant ligand covalently bonds to three $Cu^{I}(4,4'\text{-bipy})$ complexes through

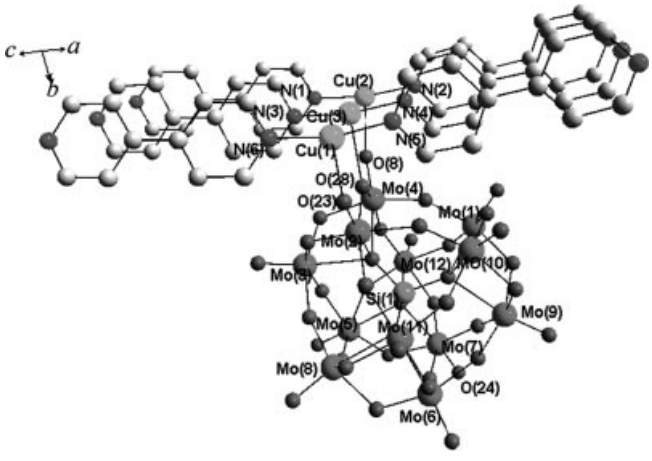

Figure 1. Representation of the molecular structure unit of **1**. The hydrogen atoms and crystal water molecules are omitted for clarity.

linearly arrayed O23, O28 and O8 atoms of the Mo_3O_{13} triad (Mo2, Mo3 and Mo4). The bond lengths around the three Cu^I ions are 2.298(8) Å (Cu1–O23), 2.383(8) Å (Cu2–O8), 2.493(8) Å (Cu3–O28), 1.888–1.898 Å (Cu1–N), 1.905–1.915 Å (Cu2–N) and 1.897–1.902 Å (Cu3–N), while the N–Cu–N angles are in the range 165.4–170.2° and the N–Cu–O angles are in the range 93.9–100.3°. There are three crystallographically independent Cu^I atoms, and each Cu^I atom adopts a "T-type" coordination geometry established by two nitrogen atoms of two 4,4′-bipy ligands and one oxygen atom of the $[SiMo_{12}O_{40}]^{4-}$ anion, which is similar to the coordination mode of $\{Cu_3(4,4'\text{-bpy})_3(H_2O)\}[PMo_{12}O_{40}(VO)_2]\cdot 5H_2O$.[19] In this way, each 4,4′-bipy ligand links two symmetrical Cu^I atoms into a one-dimensional Cu^I(4,4′-bipy) complex chain. Because each α-$SiMo_{12}O_{40}$ cluster bonds to three parallel Cu^I(4,4′-bipy) subunits, the Keggin clusters become pendants of tri-track Cu(bipy) chains, projecting towards two sides (Figure 2).

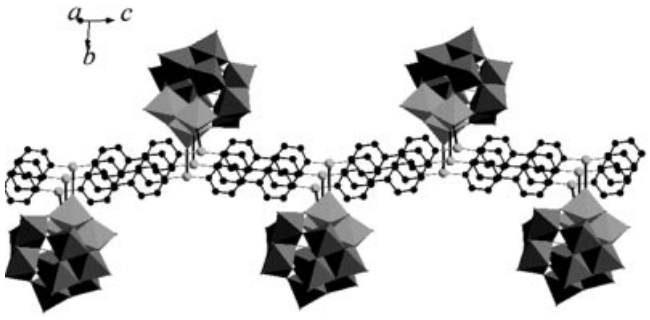

Figure 2. Combined polyhedral/wire representation of the 1D chain structure in **1**. The dark grey polyhedra represent the molybdenum polyhedra and the light grey polyhedra the Mo_3O_{13} triad bound to Cu(bipy).

The tri-track chains with POM pendants are positioned relative to each other so that the POM clusters from different chains are alternatively arranged; each POM cluster joins other neighbouring clusters through hydrogen-bonding interactions. The shortest O_d(Mo9–O18)···O_c(Mo1–O16–Mo11) distance is 2.907 Å, and the distance between Cu2 and O_d (O24) of the α-$SiMo_{12}O_{40}$ cluster of the neighbouring chain is 2.873 Å (Figure 3a), which is in the van der Waals interaction range. In this way, an interesting 2D structure is established in the manner of a "zipper" (Figure 3b).

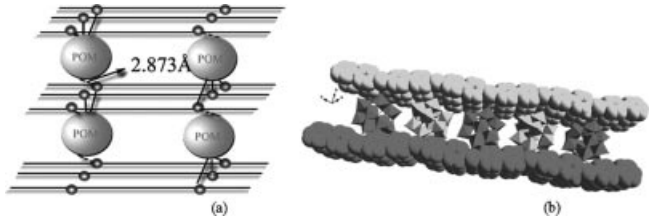

Figure 3. (a) Schematic view of part of the 2D structure in **1** with a dotted line representing the shortest distances between two adjacent chains (Cu2–O24); (b) Combined polyhedral/space filling representation of the "zipper" fashion in compound **1**. Selected bond lengths and angles for **1** are presented in Table S1.

Structural Description of 2

In the cell unit of complex **2**, there are four Cu^I ions, four 4,4′-bipy ligands and one Keggin anion $[SiW_{12}O_{40}]^{4-}$ (Figure S1). The fully oxidized Keggin structure of $[SiW_{12}O_{40}]^{4-}$ contains four W_3O_{13} units and one ordered $[SiO_4]^{4-}$ in the centre; the Si–O bonds range from 1.594(13) to 1.627(9) Å (mean 1.611 Å). The lengths of the W–O bonds can be divided into three groups: W–O_a 2.320(12)–2.387(9) Å, W–$O_{b/c}$ 1.873(8)–1.908(12) Å and W–O_d 1.691(12)–1.698(17) Å. Notably, the coordination fashion of the Cu^I(4,4′-bipy) chains to the Keggin cluster is very similar to that in complex **1** – they connect the Keggin cluster through the linearly arranged O_d···O_c···O_d atoms of the M_3O_{13} (W1, W2 and W6) triads. As shown in Figure 4a, there are three sets of linearly arranged O_d···O_c···O_d atoms at the equatorial position that can be used as coordination atoms. We can see that the significant difference between the two compounds is that in **1** only one set of O_d···O_c···O_d atoms is used (Figure 4b), while two sets of O_d···O_c···O_d atoms are used in **2**. For **2**, this means that the Keggin cluster covalently bonds to four Cu^I(4,4′-bipy) moieties through six bridging and terminal oxygen atoms of two adjacent W_3O_{13} triads at the equatorial position, which results in a rare hexadentate coordination mode in the Keggin-based coordination polymer (Figure 4c).

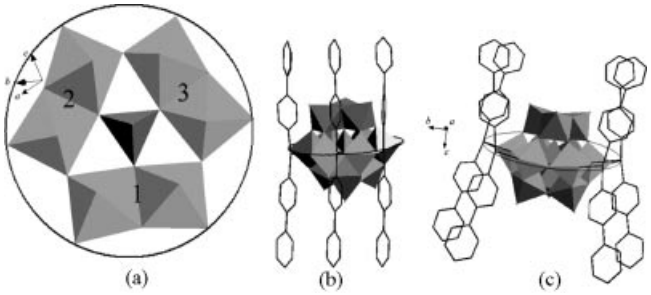

Figure 4. (a) The top view of the MO octahedra at the equatorial position; (b) Combined polyhedral/wire representation of the connection of Cu(bipy) with SiM_{12} through one set of O_d···O_c···O_d atoms in **1**, and (c) through two sets of O_d···O_c···O_d atoms in **2**. Molybdenum octahedra of the M_3O_{13} triad bound to Cu(bipy) are in light grey.

Crystal-structure analysis reveals that there are two independent Cu^I centres in **2**, in which one copper centre (Cu1) is tricoordinated by two nitrogen atoms of two 4,4′-bipy ligands and one terminal oxygen atom of the $[SiW_{12}O_{40}]^{4-}$ anion, and the other (Cu2) is tetracoordinated by two nitrogen atoms of two 4,4′-bipy ligands and two oxygen atoms (terminal and bridging oxygen) of the $[SiW_{12}O_{40}]^{4-}$ anion. The bond lengths around the Cu^I ions are 2.190 Å (Cu1–O11), 2.469(8) Å (Cu2–O10), 2.716(12) Å (Cu2–O3), 1.915–1.943 Å (Cu1–N) and 1.894–1.917 Å (Cu2–N), and the N–Cu–N bond angles are in the range 157.0–169.5° and the N–Cu–O angles in the range 97.2–105.3°. It is interesting that Cu1 and Cu2 are arrayed alternately in the 1D Cu^I chain. In this way, each 4,4′-bpy ligand links two asymmetrical Cu^I atoms into a one-dimensional Cu^I(4,4′-bipy) complex chain along the *c* axis direction. In contrast to compound **1**, each pair of adjacent α-$SiW_{12}O_{40}$ clusters covalently bonds to four

Cu^{I} chains from opposite directions to form pendants of tetra-track Cu(bipy) chains. The two adjacent POM clusters (including the bonded Cu) present an inversed relation. Owing to POM groups linked to the Cu^{I} chain with two opposite directions on the *b* axis and the inversed subunits alternately arrayed on the two sides of each pair of chains in the direction of the *c* axis, a 2D layer is extended in the [010] plane. In the 2D layer, the POM clusters and metal–organic complex chains are alternatively arranged to form a net texture with large vacancies (about 30.9×10.6 Å) (Figure 5a). The 2D layers are then stacked in a parallel staggering fashion and linked through supramolecular interactions, which lead to a 3D network frame, as shown in Figure 5b. Selected bond lengths and angles for **2** are presented in Table S2.

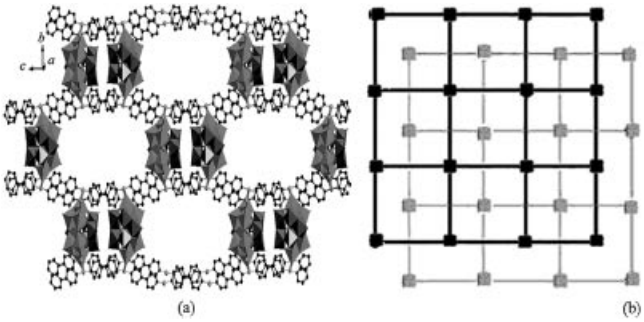

Figure 5. (a) Combined polyhedral/ball-and-stick representation of 2D layer structure in **2**. The dark grey polyhedra represent the tungsten polyhedra and the light grey polyhedra the W_3O_{13} triad bound to Cu(bipy); (b) Schematic representation of the 3D network frame in **2**.

It is noteworthy that the Cu^{I} ions show variable coordination numbers and present a nearly linear coordination with the nitrogen atoms in the bipyridine cationic chains, so they can easily accommodate one or two surface oxygen atoms of the POM to give a 2(N) + 1(O) T-type geometry (Cu1, Cu2 and Cu3 for **1**, and Cu1 for **2**), or a 2(N) + 2(O) distorted square-planar geometry (Cu2 for compound **2**), as shown in Figure 6. The O23, O28 and O8 atoms are coordinated to Cu1, Cu3 and Cu2 in **1** (Figure 6a) and the O11, and O10 and O3 atoms are coordinated to Cu1 and Cu2 in **2** (Figure 6b), respectively. The far distance between adjacent Cu atoms (Cu···Cu) make it possible that a Keggin POM is modified by bonding to co-parallel multichains of Cu(bipy) polymers through linearly arrayed O_d···O_c···O_d atoms of the M_3O_{13} triad(s). Such an unusual coordination mode has not hitherto been found in POM chemistry.

Also noteworthy are the differences in the dimension and in the number of co-parallel multichains of Cu(bipy) polymers in the two compounds, namely a tri-chain 1D structure for **1** and a di-chain 2D structure for **2**. This is perhaps due to the effect of the different volumes of the Keggin POMs. The volume of the $SiMo_{12}$ cluster is smaller than that of the SiW_{12} cluster, and in compound **1**, the unit length of a Cu(bipy) chain can just accommodate a $SiMo_{12}$ cluster, which results in an array of $SiMo_{12}$ clusters side by side. Whereas, in compound **2**, the bigger SiW_{12} clusters adopt an inversed face-to-face array, alternately arranged in pairs to form a 2D

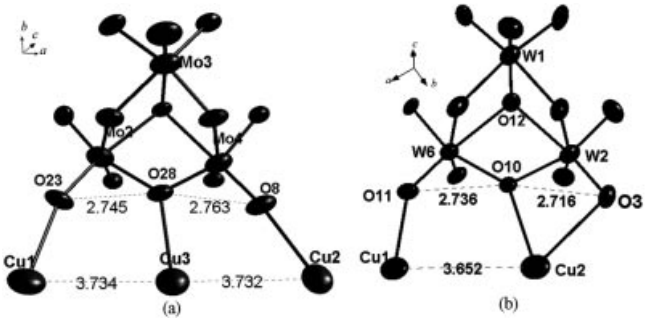

Figure 6. The view of the triad bound to multi-Cu(4,4′-bipy) with the Cu···**Cu** and O_d···O_b···O_d distances [Å] for (a) **1** and (b) **2**.

net structure with large vacancies (about 30.9×10.6 Å). The micropores are occupied by water molecules, and the solvent-accessible volume of the unit cell is estimated to be 1451.1 $Å^3$ (PLATON program[20]), which is approximately 18.5% of the unit-cell volume (7844.0 $Å^3$). The contribution of the remaining solvent-accessible voids to the unit-cell volume after the guest water molecules are taken into account is 12.9% (1010.1 per unit cell). All these parameters are greater than those of **1**, in which the solvent-accessible volume of the unit cell is 224.0 $Å^3$, which is approximately 7.30% of the unit-cell volume (3068.1 $Å^3$), and the contribution of the remaining solvent-accessible voids to the unit-cell volume after the guest water molecules are taken into account is 3.7% (114.4 per unit cell).

FTIR, XPS Spectra and TG Analyses

The IR spectra (Figure S2) exhibit prominent characteristic peaks for the α-Keggin structure at 947, 898 and 785 cm^{-1} for compound **1**, and 956, 906 and 786 cm^{-1} for compound **2**, which can be attributed to the ν_{as}(M–O_d), ν_{as}(Si–O) and ν_{as}(M–O_c–M) bands (M = Mo, W), respectively.[21] The peaks in the 1410–1610 cm^{-1} range are characteristic of the 4,4′-bipy ligands.

The bond valence sum calculations (BVS)[22] indicate that all the molybdenum and tungsten atoms are in the highest oxidation state (+6), while all the copper atoms are in the +1 oxidation state. Direct evidence for this is also provided by XPS measurements. The XPS spectra for both **1** and **2** (Figure S3) exhibit two peaks at 933.6 and 953.5 eV attributed to $Cu^{+}(2p_{3/2})$ and $Cu^{+}(2p_{5/2})$, respectively.[23] Two peaks at 232.1 and 235.7 eV can be attributed to $Mo^{+6}(3d_{5/2})$ and Mo^{+6}-$(3d_{3/2})$, respectively, for compound **1**, and a peak at 35.8 eV to W^{+6} for compound **2**.[24] Hence, addition of a proton is necessary to balance the charge of **1** in the molecular formula. Calculation of the bond strength sums was used to predict the hydrogen atom positions. Possible protonation sites are the unshared oxygen atoms (O_d) or corner- and edge-sharing oxygen atoms ($O_{b/c}$). The calculated bond strength sums indicate that the basicity of $O_{b/c}$ is stronger than that of O_d. We therefore deduce that the corner- and edge-sharing oxygen atoms ($O_{b/c}$) are protonated.

Thermogravimetric analysis (TGA) also supports the chemical composition. The TGA curves show two steps of

weight loss for compounds **1** and **2** (Figure S4). In compound **1**, the initial weight loss of 1.40% (calcd. 1.08%) from 43 °C to 236 °C corresponds to the removal of lattice water molecules, and the second weight loss of 18.1% (calcd. 18.61%) in the range 236–461 °C is ascribed to decomposition of the 4,4′-bipy ligands. The whole weight loss (19.5%) is in good agreement with the calculated value (19.73%). For compound **2**, the first weight loss of 1.60% (calcd. 1.42%) from 50 °C to 290 °C is also assigned to the removal of lattice water molecules, and the second weight loss of 15.9% (calcd. 16.4%) in the range 290–760 °C is also ascribed to decomposition of the 4,4′-bipy ligands.

Cyclic Voltammetry

To study the redox properties of compounds **1** and **2**, we used them as modifiers to fabricate chemically modified carbon paste electrode (CPE), owing to their insolubility in water and most organic solvents. As the intact Keggin skeletons in compounds **1** and **2** are still maintained, the electrochemical properties of **1** and **2** are expected to be similar to those of the parent compounds α-$H_4[SiM_{12}O_{40}]\cdot xH_2O$ (M = Mo or W).

The cyclic voltammogram of **1**-CPE was measured in 0.1 M Na_2SO_4 + 0.5 M H_2SO_4 aqueous solution in the potential range from +800 to –150 mV. There are three pairs of reversible redox peaks at +326, +217 and +8 mV [$E_{1/2} = (E_{pc} + E_{pa})/2$] (Figure 7), which correspond to three consecutive two-electron processes for Mo.[25] The values for the peak-to-peak separation between the corresponding anodic and cathodic peaks (ΔE_p) are 29 (I–I′), 38 (II–II′) and 40 mV (III–III′). These values deviate from zero, the value expected for a reversible surface redox process, perhaps because of non-ideal behaviour. It is noteworthy that the expected redox peak in the range 100–200 mV attributed to Cu^{II}/Cu^{I} was not observed, perhaps because of the overlap of the Mo^{VI}/Mo^{V} redox peak.

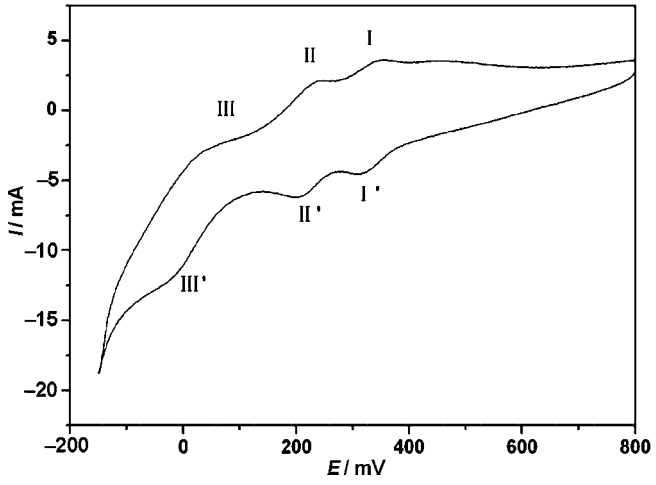

Figure 7. Cyclic voltammogram of **1**-CPE in 0.1 M Na_2SO_4 + 0.5 M H_2SO_4 aqueous solution at a scan rate of 100 mV/s.

Cyclic voltammetry on **2**-CPE was carried out in 0.1 M Na_2SO_4 + 0.5 M H_2SO_4 aqueous solution in the potential range from –700 to +300 mV. There are two pairs of reversible redox peaks at $E_{1/2}$ = –585 and –429 mV, and one irreversible peak at +131 mV (Figure 8). The values for the peak-to-peak separations between the corresponding anodic and cathodic peaks (ΔE_p) are 74 (I–I′) and 80 mV (II–II′) which shows a one-electron process. The third irreversible anodic peak is assigned to the oxidation of Cu^{I}.

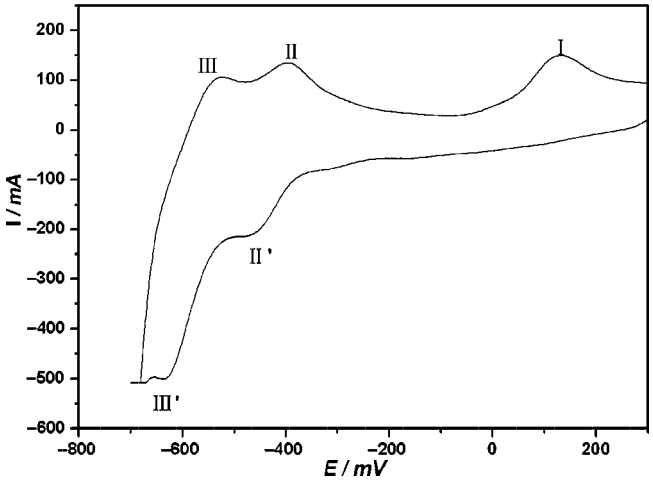

Figure 8. Cyclic voltammogram of **2**-CPE in 0.1 M Na_2SO_4 + 0.5 M H_2SO_4 aqueous solution at a scan rate of 100 mV/s.

The cyclic voltammetric behaviour of **1**-CPE as a function of scan rate (from 20 to 200 mV/s) was studied. The peak currents are proportional to the scan rates − the increase in the anodic and cathodic peak currents is almost the same, which indicates that the redox process is surface-controlled − and the exchange rate of the electrons becomes faster as the scan rate increases (Figure S5).[25b,26] The peak potentials change gradually: the cathodic peak potentials shift towards the negative direction and the corresponding anodic peak potentials towards the positive direction. The peak-to-peak separation between the corresponding cathodic and anodic peaks increases with the increasing scan rate, but the mean peak potentials do not change on the whole. In the experiment, **1**-CPE showed a higher stability than the conventional POM gel film electrode. The as-prepared electrode was stable over 300 cycle at a scan rate of 100 mV/s, and the current responses remained almost unchanged. The higher stability shows the merit of the robust POM derivatives as electrochemical active materials.

Conclusions

We have isolated two novel Keggin derivatives by using presynthesized Keggin POMs, soft Lewis acid metal Cu ions and 4,4′-bipy ligands. In **1** and **2**, the fully oxidized Keggin clusters as pendants bond to multi-Cu(4,4′-bipy) metal–organic subunits in a unique coordination fashion: Cu(4,4′-bipy) moieties are parallelly arrayed and covalently linked to the Keggin clusters through linearly arranged $O_d\cdots O_c\cdots O_d$ atoms of single M_3O_{13} triad(s). In this manner, the Keggin cluster is modified by bonding to a tri-track Cu(bipy) chain

through a set of linearly arrayed $O_d\cdots O_c\cdots O_d$ atoms of a single Mo_3O_{13} triad in compound **1**, while the Keggin cluster is modified by bonding to di-track Cu(bipy) chains through two sets of linearly arrayed $O_d\cdots O_c\cdots O_d$ atoms of two W_3O_{13} triads in compound **2**. It can be expected that there should be a Keggin POM that can be modified by bonding to multitrack Cu(bipy) chains through three sets of linearly arranged $O_d\cdots O_c\cdots O_d$ atoms from three M_3O_{13} triads. The different volumes of the Keggin POMs may have a significant influence on the dimension and on the number of co-parallel multichains of Cu(bipy) polymers in the two compounds. A tri-chain 1D "zipper" structure is seen for **1** and a di-chain 2D net-texture structure for **2**, which again highlights the effect of POM units on the self-assembly of POM-based metal–organic polymer solid materials. The successful isolation of the two novel compounds shows the possibility of extending the POM family through reasonable modification of the POM clusters by selecting suitable second metals and organic ligands. The structures of these compounds should also be helpful for understanding catalytic reactions taking place at metal oxide surfaces. Design and synthesis of other Keggin POM derivatives with such coordination modes, perhaps with a higher dimension, are currently underway to obtain novel architectures and topologies and to satisfy functional demands for inorganic–organic hybrid materials.

Experimental Section

Materials and Methods: All reagents were purchased commercially and used without further purification. Elemental analyses (C, H and N) were performed on a Perkin–Elmer 2400 CHN Elemental Analyzer, Cu, Mo and W analyses were determined by a Leaman inductively coupled plasma (ICP) spectrometer. The IR spectra were obtained on an Alpha Centaurt FTIR spectrometer in the 400–4000 cm^{-1} region with a KBr pellet. XPS analyses were performed on a VGESCALABMKII spectrometer with a Mg-K_α (1253.6 eV) achromatic X-ray source. The vacuum inside the analysis chamber was maintained at 6.2×10^{-6} Pa during analysis. The TG analyses were performed on a Perkin–Elmer TGA7 instrument under flowing N_2 with a heating rate of 10 °C/min. Cyclic voltammograms were obtained with a CHI 660 electrochemical workstation at room temperature. Platinum gauze was used as a counter electrode and Ag/AgCl electrode was used as the reference electrode. Chemically bulk-modified carbon paste electrodes were used as working electrodes.

Synthesis

{[Cu(4,4′-bipy)]$_3$[α-HSiMo$_{12}$O$_{40}$]}·1.5H$_2$O (1): The starting materials, α-$H_4[SiMo_{12}O_{40}]\cdot XH_2O$,[27] 4,4-bipy, $Cu(NO_3)_2\cdot3H_2O$, triethylamine and distilled water in a molar ratio of about 1:1:2:0.5:555, were mixed. The resulting suspension was stirred for 1 h, and the pH was adjusted to 4.3 by 1 M NaOH. The suspension was then sealed in an 18-mL Teflon-lined reactor and filled to a 60-% volume. After heating the mixture for 6 d at 160 °C, the reactor was slowly cooled to room temperature over a period of 16 h; the final pH was 4.6. Blocklike black-brown crystals of **1** were filtered, washed with water and dried at room temperature. Yield: 32% (80 mg). $C_{30}H_{28}Cu_3Mo_{12}N_6O_{42}Si$ (2507.9): calcd. C 14.36, H 1.12, Cu 7.66, Mo 45.92, N 3.35, ; found C 14.24, H 1.23, Cu 7.79, Mo 45.76, N 3.21.

{[Cu(4,4′-bipy)]$_4$[SiW$_{12}$O$_{40}$]}·3H$_2$O (2): Compound **2** was obtained in a manner similar to that illustrated for **1**, but the pH was adjusted to 5.26. Prismlike brown crystals of **2** were collected. Yield: 60% (228 mg). $C_{40}H_{38}Cu_4N_8O_{43}SiW_{12}$ (3807.19): calcd. C 12.61, H 0.99, Cu 6.67, N 2.94, W 58.00; found C 12.32, H 1.03, Cu 6.45, N 2.86, W 57.87.

X-ray Crystallographic Study: Crystal data for compounds **1** and **2** were collected on Rigaku RAXIS RAPID IP with Mo-K_α monochromatic radiation (λ = 0.71073 Å) at 293 K. The structures were solved by direct methods and refined by full-matrix least-squares on F^2 by using the SHELXTL crystallographic software package.[28] All non-hydrogen atoms were refined anisotropically. The positions of the hydrogen atoms on carbon atoms were calculated theoretically. Crystallographic data are given in Table 1. CCDC-611115 (for **1**) and

Table 1. Crystal data and structure refinements for **1** and **2**.

	1	**2**
Empirical formula	$C_{30}H_{28}Cu_3Mo_{12}N_6O_{41.5}Si$	$C_{40}H_{38}Cu_4N_8O_{43}SiW_{12}$
Formula mass	2507.9	3807.19
T [K]	293(2)	293(2)
Wavelength [Å]	0.71073	0.71073
Crystal system	triclinic	monoclinic
Space group	$P\bar{1}$	$C2/m$
a [Å]	12.963(3)	15.909(5)
b [Å]	13.571(3)	23.537(5)
c [Å]	18.034(4)	21.310(5)
α [°]	88.78	90
β [°]	87.08	100.580(5)
γ [°]	75.55	90
V [Å^3]	3068.1(13)	7844(4)
Z	1	4
$D_{calcd.}$ [mg/m^3]	2.709	3.219
Absorption coefficient [mm^{-1}]	3.499	18.678
F(000)	2358	6760
Goodness-of-fit on F^2	0.931	1.039
Final R indices[a]	R_1 = 0.0657	R_1 = 0.0570
[$I > 2\sigma(I)$][b]	wR_2 = 0.1838	wR_2 = 0.1397
R indices (all data)	R_1 = 0.0839	R_1 = 0.0828
	wR_2 = 0.1946	wR_2 = 0.1514

[a] $R_1 = \Sigma||F_o| - |F_c||/\Sigma|F_o|$. [b] $wR_2 = \Sigma[w(F_o^2 - F_c^2)^2]/\Sigma[w(F_o^2)^2]^{1/2}$.

-620041 (for **2**) contain the supplementary crystallographic data for this paper. These data can be obtained free of charge from The Cambridge Crystallographic Data Centre via www.ccdc.cam.ac.uk/data_request/cif.

Preparation of 1- and 2-CPE: 1-/2-modified carbon paste electrode [**1**-/**2**-CPE] was prepared as follows: graphite powder (48 mg) and **1**/**2** (8 mg) were mixed and ground together by an agate mortar and pestle to achieve a uniform mixture, and nujol (0.6 mL) was then added with stirring. The homogenized mixture was packed into a glass tube with a 1.2-mm inner diameter, and the tube surface was wiped with paper. Electrical contact was established with a copper rod through the back of the electrode.

Supporting Information (see footnote on the first page of this article): Tables for selected bond lengths and bond angles for compounds **1** and **2**, representation of the molecular structure unit of **2**, and XPS, IR and TG data of complexes **1** and **2**.

Acknowledgments

This work was financially supported by the National Natural Science Foundation of China (20671016). We would like to thank the referees for their comments.

[1] a) M. T. Pope, A. Müller (Eds.), *Polyoxometalate Chemistry from Topology via Self-Assembly to Applications*, Kluwer Academic Publishers, Dordrecht, **2001**; b) E. Coronado, L. Kazansky, A Müller, M. T. Pope (Eds.), *Polyoxometalate Molecular Science*, Kluwer Academic Publishers, Plenum Publishers, New York and Dordrecht, **2001**; c) M. T. Pope, *Heteropoly and Isopoly Oxometalates*, Springer-Verlag, Berlin, **1983**.
[2] a) C. L. Hill, *Chem. Rev.* **1998**, *98*, 1–2; b) A. Proust, P. Gouzerh, *Chem. Rev.* **1998**, *98*, 77.
[3] M. Pohl, Y. Lin, T. J. R. Weakley, K. Nomiya, M. Kaneko, H. Weiner, R. G. Finke, *Inorg. Chem.* **1995**, *34*, 767–777.
[4] E. Burkholder, V. Golub, C. J. O'Connor, J. Zubieta, *Inorg. Chem. Commun.* **2004**, *7*, 363–366.
[5] Y. Xu, J. Q. Xu, K. L. Zhang, Y. Zhang, X. Z. You, *Chem. Commun.* **2000**, *6*, 153–154.
[6] X. L. Wang, C. Qin, E. B. Wang, Z. M. Su, Y. G. Li, L. Xu, *Angew. Chem. Int. Ed.* **2006**, *45*, 7411–7414.
[7] S. Masahiro, M. H. Dickman, M. T. Pope, *Angew. Chem. Int. Ed.* **2000**, *39*, 2914–2916.
[8] a) L. S. Felices, P. Vitoria, J. M. Gutiérrez-Zorrilla, S. Reinoso, P. Vitoria, L. Lezama, *Chem. Eur. J.* **2004**, *10*, 5138–5146; b) S. Reinoso, P. Vitoria, J. M. Gutiérrez-Zorrilla, L. Lezama, J. I. Beitia, *Inorg. Chem.* **2005**, *44*, 9731–9741; c) S. Reinoso, P. Vitoria, L. S. Felices, J. M. Gutiérrez-Zorrilla, *Chem. Eur. J.* **2005**, *11*, 1538–1548.
[9] C. Ritchie, E. Burkholder, P. Kögerler, L. Cronin, *Dalton Trans.* **2006**, *14*, 1712–1714.
[10] Y. P. Ren, X. J. Kong, L. S. Long, R. B. Huang, L. S. Zheng, *Cryst. Growth Des.* **2006**, *6*, 572–576.
[11] Y. P. Ren, X. J. Kong, X. Y. Hu, M. Sun, L. S. Long, *Inorg. Chem.* **2006**, *45*, 4016–4024.
[12] J. X. Chen, T. Y. Lan, Y. B. Huang, C. X. Wei, Z. S. Li, *J. Solid State Chem.* **2006**, *179*, 1904–1911.
[13] H. Y. An, D. R. Xiao, E. B. Wang, Y. G. Li, Z. M. Su, L. Xu, *Angew. Chem. Int. Ed.* **2006**, *45*, 904–908.
[14] a) D. Ghosh, R. Mukherjee, *Inorg. Chem.* **1998**, *37*, 6597–6605; b) D. A. Rochcliffe, A. E. Martelldummy Martell, *J. Mol. Catal. A* **1995**, *99*, 101–105.
[15] a) L. S. Felices, P. Vitoria, J. M. Gutiérrez-Zorrilla, L. Lezama, S. Reinoso, *Inorg. Chem.* **2006**, *45*, 7748; b) C. Z. Lu, C. D. Wu, H. H. Zhuang, J. S. Huang, *Chem. Mater.* **2002**, *14*, 2649–2655; c) H. Jin, C. Qin, Y. G. Li, E. B. Wang, *Inorg. Chem. Commun.* **2006**, *9*, 482–485.
[16] a) C. D. Wu, C. Z. Lu, H. H. Zhuang, J. S. Huang, *Inorg. Chem.* **2002**, *41*, 5636–5637; b) C. M. Liu, D. Q. Zhang, D. B. Zhu, *Cryst. Growth Des.* **2005**, *5*, 1639–1642.
[17] C. M. Liu, D. Q. Zhang, M. Xiong, D. B. Zhu, *Chem. Commun.* **2002**, 1416–1417.
[18] A. S. J. Wery, J. M. Gutierrez-Zorrilla, A. Luque, P. Vitoria, P. Roman, M. Martinez-Ripoll, *Polyhedron* **1998**, *17*, 1247–1251.
[19] Z. Y. Shi, X. J. Gu, J. Peng, X. Yu, E. B. Wang, *Eur. J. Inorg. Chem.* **2006**, 385–388.
[20] A. L. Spek, *PLATON, A Multipurpose Crystallographic Tool*, Utrecht University, Utrecht, The Netherlands, **1998**.
[21] R. Thouvenot, M. Fournier, R. Franck, G. Rocchiccioli-Deltche, *Inorg. Chem.* **1984**, *23*, 598–605.
[22] I. D. Brown, D. Altermatt, *Acta Crystallogr., Sect. B: Struct. Sci.* **1985**, *41*, 244–247.
[23] Y. H. Feng, Z. G. Han, J. Peng, X.-R. Hao, *J. Mol. Struct.* **2005**, *734*, 171–176.
[24] Z. G. Han, Y. L. Zhao, J. Peng, A. X. Tian, Q. Liu, J. F. Ma, E. B. Wang, N. H. Hu, *CrystEngComm* **2005**, *7*, 380–387.
[25] a) M. Sadakane, E. Steckhan, *Chem. Rev.* **1998**, *98*, 219–237; b) Z. G. Han, Y. L. Zhao, J. Peng, Y. H. Feng, J. N. Yin, Q. Liu, *Electroanalysis* **2005**, *17*, 1097–1102; c) Z. G. Han, Y. L. Zhao, J. Peng, Q. Liu, E. B,Wang, *Electrochim. Acta* **2005**, *51*, 218–224.
[26] M. T. Pope, E. Papaconstantinou, *Inorg. Chem.* **1967**, *6*, 1147–1152.
[27] C. R. Deltcheff, M. Fournier, R. Franck, R. Thouvenot, *Inorg. Chem.* **1983**, *22*, 207–216.
[28] a) G. M. Sheldrick, *SHELX-97, Program for Crystal Structure Refinement*, University of Göttingen, Germany, **1997**; b) G. M. Sheldrick, *SHELXL-97, Program for Crystal Structure Solution*, University of Göttingen, Germany, **1997**.

Received: October 29, 2006
Published Online: February 16, 2007

